Available online at www.sciencedirect.com
ScienceDirect
Journal of Applied Geophysics 60 (2006) 165–178
JOURNAL OF APPLIED GEOPHYSICS
www.elsevier.com/locate/jappgeo

Correlations between geotechnical and electrical data: A case study at Garchy in France

Philippe Cosenza [a,b,*], Eric Marmet [a], Faycal Rejiba [a], Yu Jun Cui [c], Alain Tabbagh [a,b], Yvelle Charlery [a]

[a] UMR 7619 Sisyphe, Université Pierre et Marie Curie, Paris, France
[b] Institut de Sciences et Technologie (IST), Université Pierre et Marie Curie, Paris, France
[c] CERMES, ENPC-LCPC, Institut Navier, Champs-sur-Marne, France

Received 5 September 2005; accepted 28 February 2006

Abstract

Geophysical (Electrical Resistivity Tomography, Ground Penetrating Radar profiles and seismic refraction) and geotechnical (dynamic penetrometer, in situ vane test) surveys were carried out at Garchy (Nièvre, France). The main objective of this study was to establish qualitative and quantitative correlations between electrical and geotechnical data from this site in a simple geological context.

Concerning qualitative correlations, geotechnical tests and Electrical Resistivity Tomography sections are consistent with a three-layers model: a fine soil with a significant clay fraction sandwiched between a low moisture sandy soil and oolitic limestones. Despite the usual difficulty to locate clearly interfaces in inverted ERT sections, both methods provide consistent depths of the substratum top. Moreover, this study confirms that correlations between reflectors of GPR profiles and vertical geotechnical property variations are mainly explained by vertical water content changes.

As far as quantitative correlations are concerned, no clear relationship between cone resistance and inverted resistivity extracted from ERT sections has been observed. Nevertheless, if we do not consider the upper sandy soil composed with gravels, the couple inverted resistivity–cone resistance would be a lithological discriminator. This lithological discrimination is enhanced when inverted resistivity values obtained from extracted 1D soundings are considered. This original result should be validated in other sites. Moreover, a satisfactory quantitative correlation between inverted resistivity values and measured water content values has been obtained; this correlation demonstrates once more that resistivity is a good indirect predictor of water content.

Keywords: Geotechnical tests; Electrical tomography; Ground Penetrating Radar; Water content

1. Introduction

Proper design and successful construction of any structure require an accurate determination of the engineering properties of the soils at the site. For this purpose, geotechnical field tests (cone penetration test, dynamic and static cone penetration test, in situ vane

* Corresponding author. Université Pierre et Marie Curie, UMR Sisyphe, Case 105 — Tour 46/56-3ème étage, 4, place Jussieu, 75252 Paris Cedex 05, France.
E-mail address: cosenza@ccr.jussieu.fr (P. Cosenza).

0926-9851/$ - see front matter © 2006 Elsevier B.V. All rights reserved.
doi:10.1016/j.jappgeo.2006.02.003

shear test, pressiometer etc.) are performed in order to obtain necessary data for the soils.

Nevertheless, these tests can be time-consuming and expensive: the number of geotechnical tests in a site investigation is commonly limited. Therefore, it is desirable to extrapolate and/or interpolate consistent 1D geotechnical data from geophysical measurements that are more rapid and non-invasive.

In offshore context, a methodology, which allows integrating seismic and geotechnical data is now available (e.g. Nauroy et al., 1998; Puech et al., 2000). This is mainly due to (i) a large number of empirical and theoretical relationships between the seismic and geotechnical properties of marine sediments in the literature, (ii) an improvement of seismic acquisition systems in order to perform very high resolution seismic surveys. In the onshore context, seismic cone penetration test (CPT) shows very promising results (Ghose and Drijkoningen, 2000). Moreover, analysis of seismic surface waves can also provide a significant contribution for integrating seismic and geotechnical properties (Abraham et al., 1998).

Considering other geophysical methods, the attempts to relate geotechnical properties to electrical data are rare: the interdependence between these properties is not well understood in a fundamental basis. Moreover, literature shows apparently some contradictory results. Analysis of data from Dover Air Force Base site (USA) has revealed relationships between soil types determined from mechanical properties measured by CPT and the electrical properties, i.e. resistivity and dielectric permittivity, obtained from logging (Endres and Clement, 1998). The authors suggest that these relationships may provide a petrophysical basis for combining information from CPT and geophysical techniques governed by electrical properties. The site was located on a level, grass field where the underlying sediments are part of a Pleistocene fluvial system with lithologies ranging from clayey silt to coarse sand units.

Braga et al. (1999) studied the relationship between blow counts N from the Standard Penetration Test (SPT), the chargeability C from Induced Polarization (IP) survey and resistivity values inverted from Vertical Electrical Soundings (VES). The geophysical survey was made in the Rio Claro and Corumbatai formations of the sedimentary basin of Parana. The Rio Claro Formation consists of poorly consolidated sandy–clay sediments; the Corumbatai formation comprises claystones, sandy siltstones and clay siltstones. The authors found that (i) there is no relationship between N and C; (ii) the inverted resistivity is weakly correlated with N.

In the Le Havre site (France), Lagabrielle et al. (2000) showed that resistivity profiling in sea water environment can describe the offshore alluvium stratigraphy and give its characteristics in terms of thickness and mechanical strength. In the Nakdong river plain site (Korea), Giao et al. (2003) did not observe relationships between geotechnical parameters (Plasticity index, water content and unit weigh) and resistivity values measured in the field and in laboratory from samples taken from Pusan clays.

In fact, these results are not to be compared directly with each other for different reasons: (i) The geotechnical parameters involved in these studies are not directly related with each other. For instance, cone strength measured from SPT and CPT may be different at the same site. Moreover, Plasticity Index is a specific parameter: it is only measured for fine soils. (ii) The geological backgrounds and the experimental techniques (logging, laboratory or field tests) are also different in the previous studies, which make the comparisons difficult, partly due to scale effects.

Consequently, to our opinion, a synthetic overview and a deep understanding of the relationships between geotechnical parameters and the electrical properties, i.e. electrical resistivity and dielectric permittivity are not available today. We are convinced that this deep understanding has to be obtained following two complementary approaches: (a) the first one is to perform laboratory studies for which lithological and petrophysical parameters can be easily controlled; and (b) the second is to obtain more datasets obtained from different and well characterized sites and different acquisition parameters are required.

Following the second approach, the main objective of this paper is to provide a significant amount of data collected from the same site to analyse this set in order to establish correlations. This paper is divided into three parts. The first part is devoted to the methodology used to collect geotechnical and geophysical data at the site. The second and the third parts deal with the qualitative and the quantitative analysis of this dataset respectively.

2. Methodology

2.1. Site and equipment description

The study site is located at Garchy (Nièvre) in the southeast part of the sedimentary basin of Paris. The underlying formations which are concerned up to a few dozens of meters depth are (i) Pliocene alluvial formations with lithologies ranging from clayey silt to coarse sand units and (ii) Jurassic (upper oxfordian)

oolithic limestones. The interface between these two geological units provides a preferential target for geotechnical and geophysical methods. The water table is estimated in this area between 5 and 11 m depth (Menot et al., 1997).

This site, located near the former Centre de Recherche Geophysique (CRG), presents at least five advantages: (i) a large open ground is accessible; (ii) there is neither subsurface metal objects (e.g. buried pipes) nor ancient building remains; (iii) no topographic correction is necessary; (iv) the electrical properties of subsurface soils are known to induce significant vertical changes and interfaces; (v) the geological background is quite simple (e.g. sedimentary context).

Two geotechnical devices were used: (a) in situ vane shear test, (b) dynamic cone penetration test (Fig. 1). In situ vane shear test is best suited for the determination of shear strength of saturated soft soils, especially fine soils (silts and clays). This device consists of pushing a four-bladed vane in the soil and rotating it until a cylindrical surface fails by shear. The torque required to induce the failure is measured and converted to an undrained shear strength c_u usually expressed in kPa. The undrained shear strength c_u is given by the following equation (e.g. Venkatramaiah, 1993):

$$c_u = \frac{T}{\pi D^2 \left(\frac{H}{2} + \frac{D}{6}\right)} \quad (1)$$

where T is the torque at failure; D is the overall diameter of the vane and H is the height of the vane.

The dynamic cone penetrometer test is recommended in preliminary investigations and to control the mechanical strength of the soils. It consists of a cone, driving rods, driving head and a hammer. A lightweight device was used and no hoisting equipment was required. During the experiment, the cone is driven into the soil by allowing the hammer to fall freely through 500 mm each time. The number of blows for every 200 mm penetration of the cone is recorded and converted to a cone resistance q_d using the Dutch formula:

$$q_d = \frac{M}{e(M + M')} \frac{MH}{A} \quad (2)$$

where M is the weight of the striking mass (e.g. the hammer, 10 kg weight); M' is the weight of the struck mass; e is the average penetration depth; H is the height corresponding to the hammer fall (e.g. 500 mm). From a practical point of view, the cone resistance, usually expressed in MPa, is calculated with a simplified form of Eq. (2):

$$q_d = CN \quad (3)$$

where N is the number of blows for every 200 mm penetration and C a predefined constant which is function of M, M', e, H and g.

It should be mentioned that these geotechnical field tests may not be representative of a classical site investigation for determining the engineering properties. For instance, CPT tests are often preferred because they allow to characterize lithologies. Moreover, pressumeter tests which are widely used in France, give fundamental parameters for soil strength and settlement analysis. Despite of this drawback, the

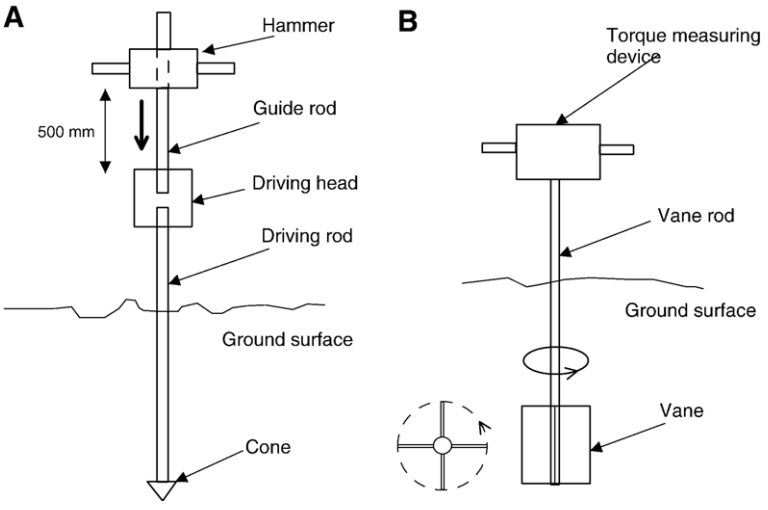

Fig. 1. Geotechnical devices. A: Dynamic cone penetration test. B: In situ vane shear test.

in situ vane shear test and this dynamic cone penetration test offer two advantages: they are simple and lightweight apparatus and no preliminary borehole is required.

In order to compare electrical properties and the data provided by the previous geotechnical tests, two geophysical methods were used: Electrical Resistivity Tomography (ERT) and Ground Penetrating Radar (GPR) profiling technique. The 2D electrical imaging surveys were carried out with a multielectrode and multicable system: a SYSCAL R1+ resistivity meter, a multiplexer, with two multinodes for 32 electrodes. No external power supply was used. The GPR measurements were collected with a PulseEKKO 100 radar with three shielded antennas: 50, 100 and 200 MHz. The acquisition parameters of both methods have been defined after a preliminary electrical survey of the site.

2.2. Results of the preliminary electrical survey

This preliminary survey consists of Wenner mapping, EM31 mapping and VES. The main objectives were: (i) To identify the ability of the electrical techniques to distinguish different geological units, and to refine the resistivity characteristics of these units; (ii) To optimize the acquisition parameters of the geophysical imaging techniques, as mentioned previously.

The mapping with the Wenner array, with a 5 m separation is given in Fig. 2A. In this figure, the apparent resistivity values show a general decrease towards the east, from about 200 Ω m to less than 20 Ω m. EM31 mapping confirmed this trend (Fig. 2B).

VES curves obtained from 12 soundings with an alpha Wenner array suggested a three-layers organization: a conductive formation (about 4 m thick in average, with resistivity values ranging from 20 up to 75 Ω m) sandwiched between a resistive top layer (about 0.7 m thick in average, with a resistivity value ranging from 150 to 230 Ω m) and a resistive substratum (resistivity values ranging from 150 to 550 Ω m). From the geological background of the site, the top layer and the middle layer are associated with alluvial formations. The middle layer could be identified as so-called Bourbonnais clays widespread in the area. The substratum layer is related to a part of the Jurassic limestones likely weathered at its top. Hereafter, the top layer, the middle layer and the substratum will be called formation A, B and C respectively (Fig. 3).

In addition to the electrical surveys, sampling was performed using a soil auger and confirmed the lithologies inferred previously. They also show that the layer A is sometimes constituted of gravels, which could disturb the geotechnical tests.

2.3. Data acquisition

On the basis of this preliminary survey, two lines representative of this site were chosen: the lines 15 and 25 in the local reference (see Fig. 2A and B). The direction (north–south) of these lines has been chosen in order to minimize the effect of lateral (horizontal) variations in resistivity oriented east–west, observed in the maps. In line 150, GPR data were collected preferentially since GPR technique works best in electrically resistive environments. Moreover, electrical mapping shows no important apparent resistivity lateral change. In line 25, significantly high thickness of clayey soils was expected.

In order to detect both interfaces with a satisfactory resolution, separations of 0.5 and 1 m between each electrode for the ERT have been chosen. This choice is a compromise between (a) and the best spatial resolution in order to detect the shallowest interface (layer A/layer B) and (b) an optimal depth of investigation in order to identify the second interface (layer B/layer C). For our system of 32 electrode and an alpha Wenner array, the "equivalent depth of investigation" (Edwards, 1977) is equal to 2.7 m (5.4 m respectively) considering an electrode spacing of 0.5 m (1 m respectively). Alpha Wenner arrays were used since no strong horizontal variations were expected at the scale of a pseudo-section.

The labels of the 32 electrode profiles and their location are given in Table 1. Note that both lines, line 150 and line 25, were partially covered by ERT profiles. This choice resulted from the available duration for the survey and the geotechnical results as it will be discussed further.

Concerning GPR profiles, no specific antenna was preferred but the line 150 was investigated preferentially as it was recommended. GPR profiles have been performed in a "cross-line" bistatic configuration. The acquisition parameters are given in Table 2.

In addition to these electrical surveys, seismic refraction profiles in lines 150 and 25 have been carried out in order to improve the interpretations and thus the correlations. The acquisition was made using a 24-channel Mark VI seismograph (ABEM) and vertical 4.5 Hz geophones. A 6 kg sledge-hammer was used as an impulsive source.

Concerning the geotechnical data acquisition, in situ vane shear tests and dynamic cone penetration tests were

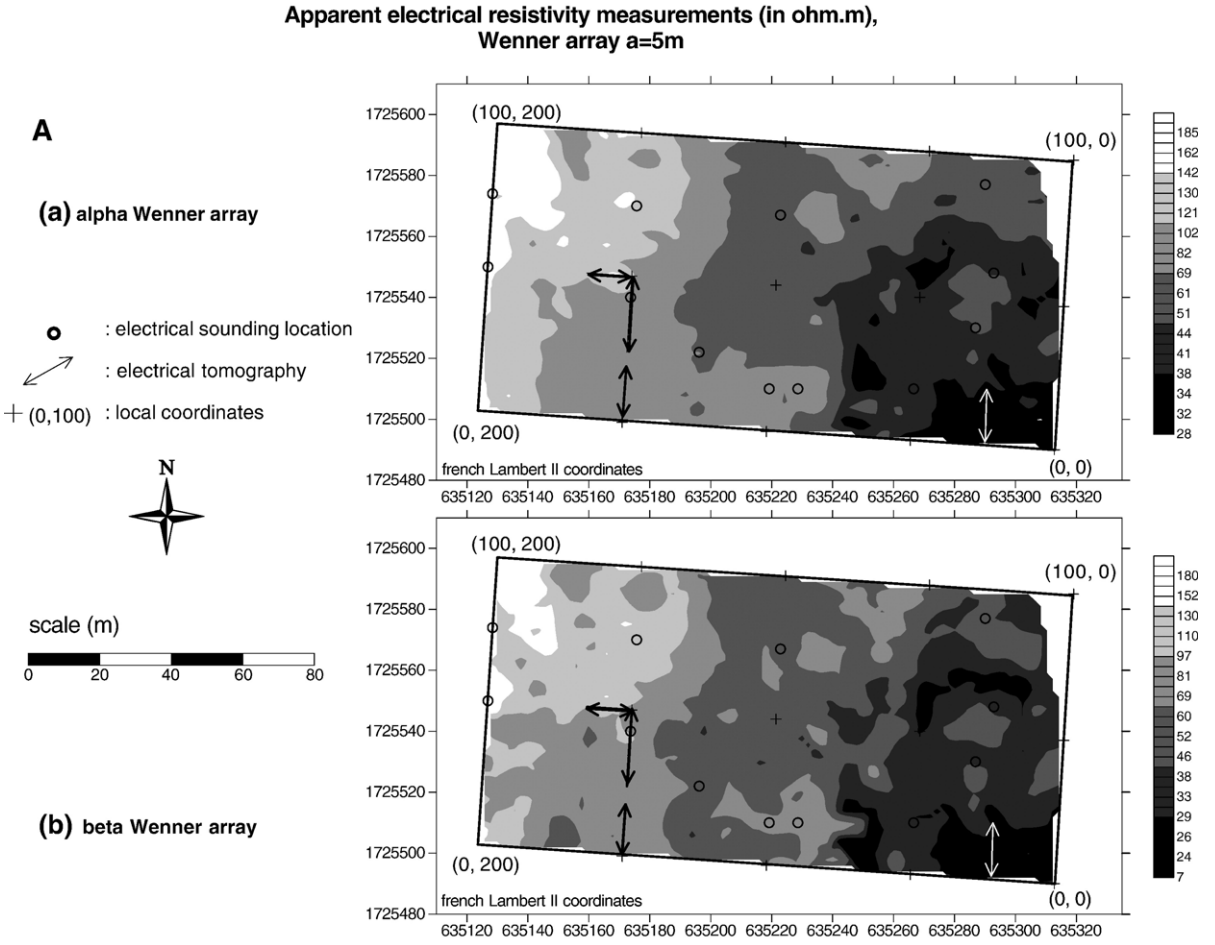

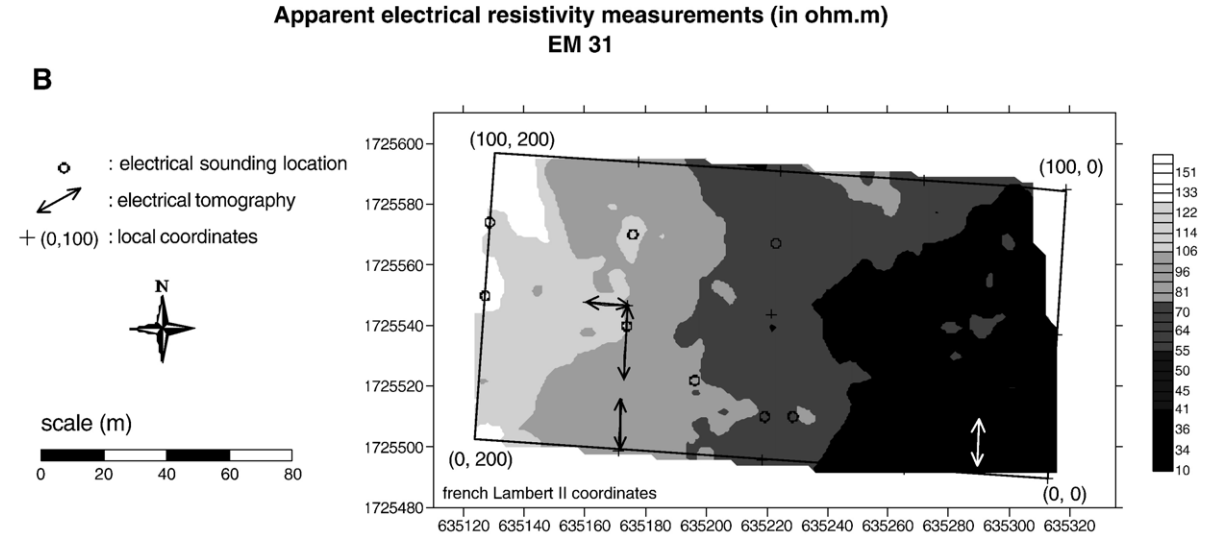

Fig. 2. Electrical maps following two configurations (alpha Wenner and beta Wenner) and approximate locations of resistivity profiles and vertical electrical soundings.

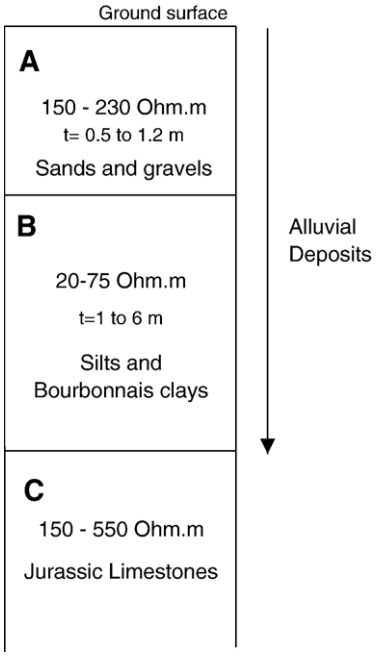

Fig. 3. Geoelectrical model obtained from VES.

initially designed alternatively every 4 m in line 150. But, the existence of gravels in the top layer A has limited the number of geotechnical tests: maximum depth of numerous tests was smaller than 50 cm. These tests have not been considered further. Consequently, the ERT profiles in line 150 were located preferentially on successful geotechnical soundings. Note that dynamic cone penetration test was often preferred since it was the most rapid geotechnical test.Hereafter in the figures, these geotechnical soundings are labelled according to their location in the profile and their type. For instance, the test P44 in line 150 indicates a penetrometer experiment located at the point $x=44$ m $y=150$ m in local coordinates.

Table 1
Location and electrode separation of the ERT profiles (see also Fig. 2)

Line	ERT profile	Label	Electrode separation (m)
Line 150	x0.5–16y150,	1	0.5
	x2.5–18y150,	2	
	x24–39.5y150,	3	
	x34.5–50y150,	4	
	x50y150–165.5 [a]	5	
	x14–45y150,	6	1
	x19–50y150	7	
Line 25	x–1–14.5y25	8	0.5

The 32 electrodes profiles were labelled according to the local coordinates (in the line) of the extreme electrodes. For instance, the ERT profile x0.5–16y150 means that both extreme electrodes in the single spread of 32 electrodes were located between the points $x=0.5$m $y=150$ m and $x=6$ m $y=150$ m in the local reference.

[a] This profile has been carried out perpendicular to the line 150.

Table 2
Acquisition parameters used for the GPR profiles

Antenna frequency (MHz)	50	100	200
Antenna separation (m)	2	1	0.5
Trace interval (m)	0.5	0.2	0.1
Sampling period (ps)	400	800	800
Vertical stack	16	16	16

3. Qualitative correlations between electrical and geotechnical data

3.1. ERT vs geotechnical data

The ERT results with the associated geotechnical tests at lines 150 and 25 are presented in Figs. 4–8. The ERT data have been inverted using the software package RES2DINV (Locke 2004). The inversion process used in this forward modelling program is based on a smoothness-constrained (or Occam) least-squares method (e.g., De Groot-Hedlin and Constable, 1990). The 2D-model used in the forward modelling program, which consists of a number of rectangular blocks, is automatically generated. The depth of the bottom raw of blocks is set to be approximately equal to the "equivalent depth of investigation"(Edwards, 1977) calculated with the largest electrode spacing. We chose the following inversion options:

(a) The "conventional" smoothness-constrained least-squares method or l_2 norm inversion method that leads to produce a model with a smooth variation of resistivity values. In the geological context and at the considered spatial scale, no sharp interfaces (fault, dyke, etc.) between the different units were expected.
(b) A model refinement that allows to get model cells with width of half the unit electrode spacing, in order to obtain more accurate results when large resistivity changes are expected near the ground surface.
(c) A maximum number of iterations equal to 5 for the inversion process.

For the whole set of profiles, the RMS errors we obtained were less than 1.5%. During the inversion progress, the apparent resistivity contrast less than 20/1 (ratio of the maximum apparent resistivity to the minimum apparent resistivity). Consequently, on the basis of the low RMS error values and the calculated

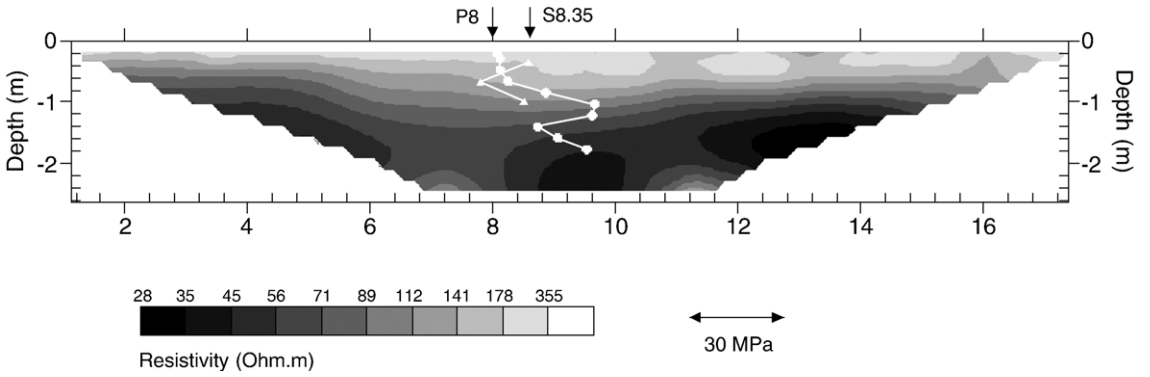

Fig. 4. Inverted resistivity cross-section for a part of Line 150 (profile 1 and profile 2) with associated geotechnical tests.

resistivity contrast, our initial mesh grinds were considered acceptable: no additional mesh refinement was required.

All the results confirm roughly the geoelectric model given in Fig. 3: a conductive layer between two more resistive layers.

Concerning the geotechnical results, a major part of the investigations shows two features: (i) a first peak of cone resistance q_d located at about 1 m depth (Figs. 4–6 and 8) and (ii) a steep increase of cone resistance at about 2.5 m depth (Fig. 5). The first feature, the q_d peak may be explained by:

- A lithological interface between the layer A (sands and gravels, i.e. coarse dry soils) and the layer B (silts and clays, i.e. fine wet soil).
- A local concentration of gravels that have been observed in the field from the samples collected by the auger.
- A vertical change of water content. This point will be discussed further.

This q_d peak seems to be associated with a decrease of the undrained shear strength (Fig. 8) and it is qualitatively well correlated with the transition between the shallow high resistivity values and the low resistivity values associated with clayey soils (see Figs. 5, 6 and 8; in Fig. 6 the white dashed line corresponds to the isovalue of resistivity 79 Ω m).

The steep increase of cone resistance at about 2.5 m depth (Figs. 5 and 7) is likely related to the top of layer C (limestones). It is well correlated to the increase of resistivity in the inverted pseudo-sections (see in Fig. 5, the white dashed line corresponds to the isovalue of resistivity 79 Ω m).

Both methods, ERT and penetration tests, predict a significant raising of the limestone top at about $x=43$ m in the line 150 (Figs. 5 and 6). This steep variation of the

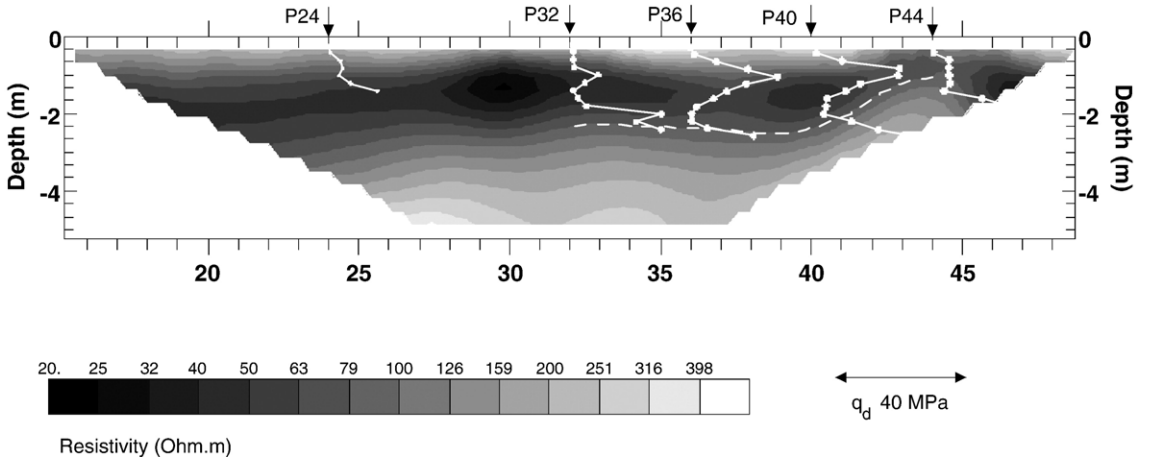

Fig. 5. Inverted resistivity cross-section for a part of Line 150 (profile 6 and profile 7) with associated geotechnical tests. Electrode separation is 1 m. The white dashed line corresponds to the isovalue of resistivity 79 Ω m.

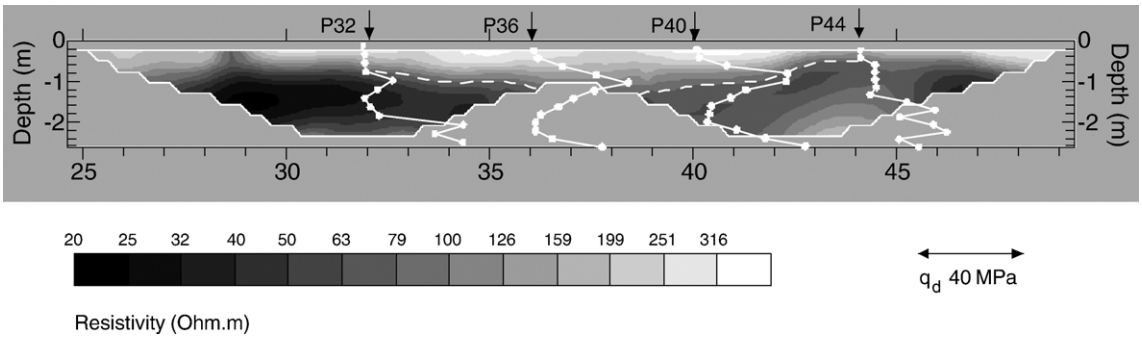

Fig. 6. Inverted resistivity cross-section for a part of Line 150 (profile 3 and profile 4) with associated geotechnical tests. Electrode separation is 0.5 m. The white dashed line corresponds to the isovalue of resistivity 79 Ω m.

bedrock topography at the same location can be also observed in the electrical map (Fig. 2A) with the beta Wenner array that is more sensitive to lateral effects. The results of the refraction survey confirm also this steep change of topography: clear delays of the trend of the travel–times curves are observed at $x=43$ m (Fig. 9). Moreover, the interpreted velocity values and the cone resistance values suggest that layer C is likely a partly saturated and weathered limestone (Meyer De Stadelhofen, 1991; Venkatramaiah, 1993).

Consequently, this comparison between all these methods proves once more that the ERT is an interesting tool to estimate the depth of bedrock covered BY superficial clay deposits and to determine the thickness of the latter (e.g. Vickery and Hobbs, 2003). In this context, it should be noted that using geotechnical tests may be useful to calibrate the interface depths given by an unconstrained ERT inversion.

3.2. GPR vs. geotechnical data

In displaying GPR data, we observed that the suitable data for establishing correlations had been obtained with the 200 MHz antennas. Indeed, radar profiles collected with 50 and 100 MHz antennas had a too low vertical resolution.

The data processing of the GPR traces consisted mainly in a "Dewow" correction and the application of an adaptive gain such as an AGC. In order to convert times into depths in GPR sections, velocities have been estimated from radar logging carried out with boreholes located at $x=5$ m and $x=9$ m at line 25 and from the sides of hyperbolae related to diffractions. A mean velocity of 0.07 m/ns has been obtained. This value corresponds to a dielectric constant value of 18.4 that is representative of a wet soil.

Figs. 10 and 11 show the GPR sections with 200 MHz antennas and the corresponding geotechnical tests (in red) at lines 25 and 150. The depths marked on the right-hand vertical axis in the figures have been calculated using the mean velocity of 0.07 m/ns. In Fig. 10, a good qualitative correlation between a steep increase of q_d resistance and a strong reflection drawn in blue can be observed. Moreover, high values of undrained cohesion at $x=9$ m in the same figure seems also to be associated with a strong event, drawn also in blue, located

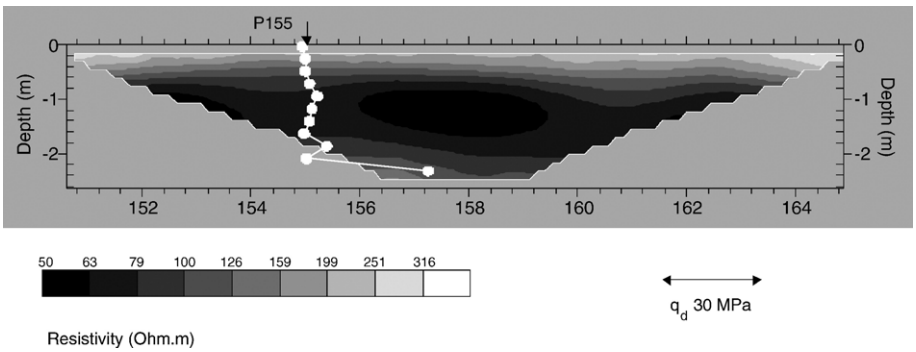

Fig. 7. Inverted resistivity cross-section for a profile perpendicular to Line 150 (profile 5) with associated geotechnical tests.

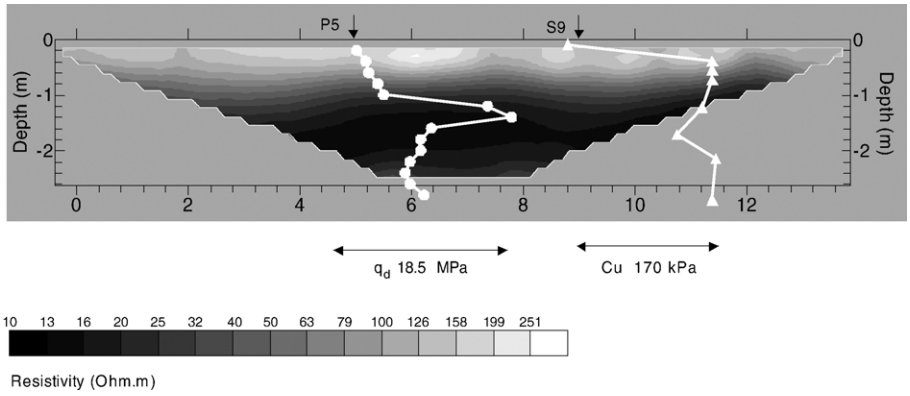

Fig. 8. Inverted resistivity cross-section for Line 25 (profile 8) with associated geotechnical tests.

approximately at the same depth. The origin of these qualitative correlations has been understood by measuring the water content of samples collected from the borehole at $x=9$ m. Fig. 12 shows that the increase of resistance q_d is quite well corroborated with an increase of water content likely associated with low resistivity values (Fig. 8) likely related to an high clay fraction of this formation. Thus, the existence of such a clay formation generates two effects: (a) a mechanical effect and (b) an electromagnetic effect.

Considering the first effect, during the mechanical penetration, when the cone meets the wet clayey formation, a significant pore pressure build-up Δu is generated due to the low permeability of a clayey formation. This pore-pressure build-up leads to an increase of the apparent soil strength and thus induces a q_d peak. This phenomenon in clayey soils is well known in geotechnical engineering when cone penetration tests are used and the duration required to dissipate Δu depends on the ability of drainage offered by the soil

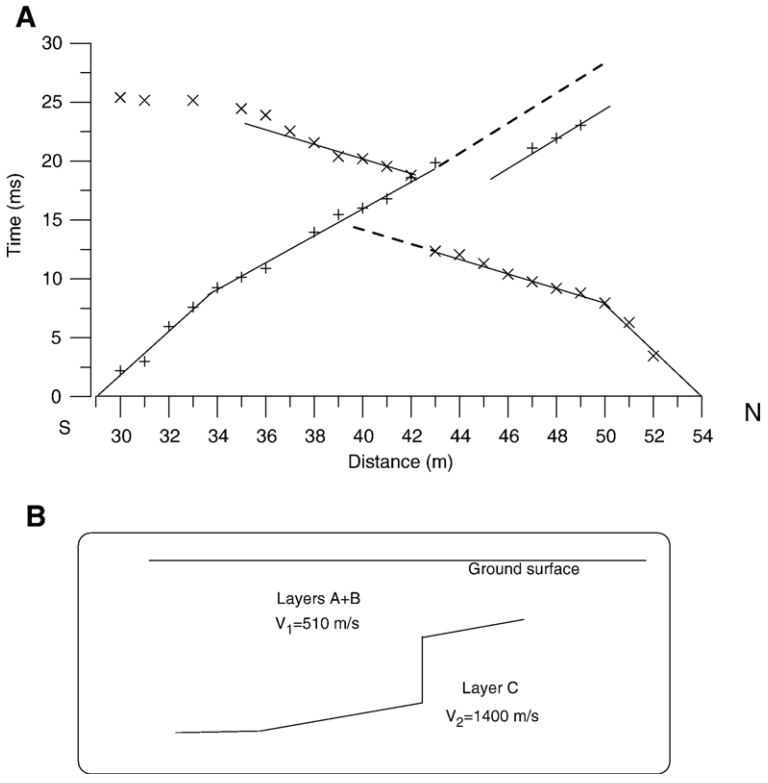

Fig. 9. A: Time–distance curves in a refraction survey located at Line 150. B: the corresponding geological model.

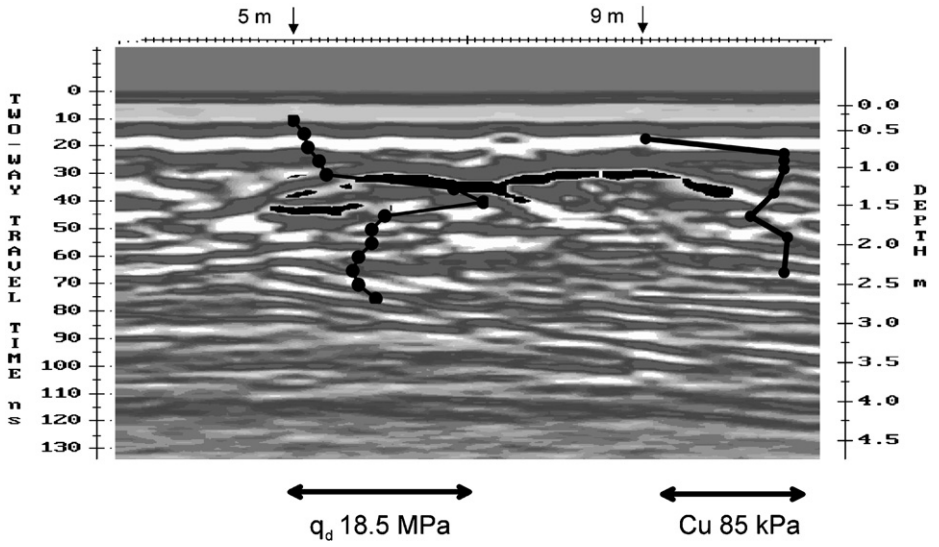

Fig. 10. Radar section at line 25 (200 MHz). The corresponding geotechnical tests are in red. Strong reflections drawn in blue are correlated with the increase (resp. decrease) of the cone resistance (resp. the undrained shear strength). (For interpretation of the references to colour in this figure legend, the reader is referred to the web version of this article.)

permeability and the cone itself (e.g. Filliat, 1981). In this context, a static penetration test coupled with a pore-pressure measurement would be useful to study such a phenomenon. Considering the electromagnetical effect, the contrast between the dielectric permittivity of the wet clayey soil and above the rather dry material

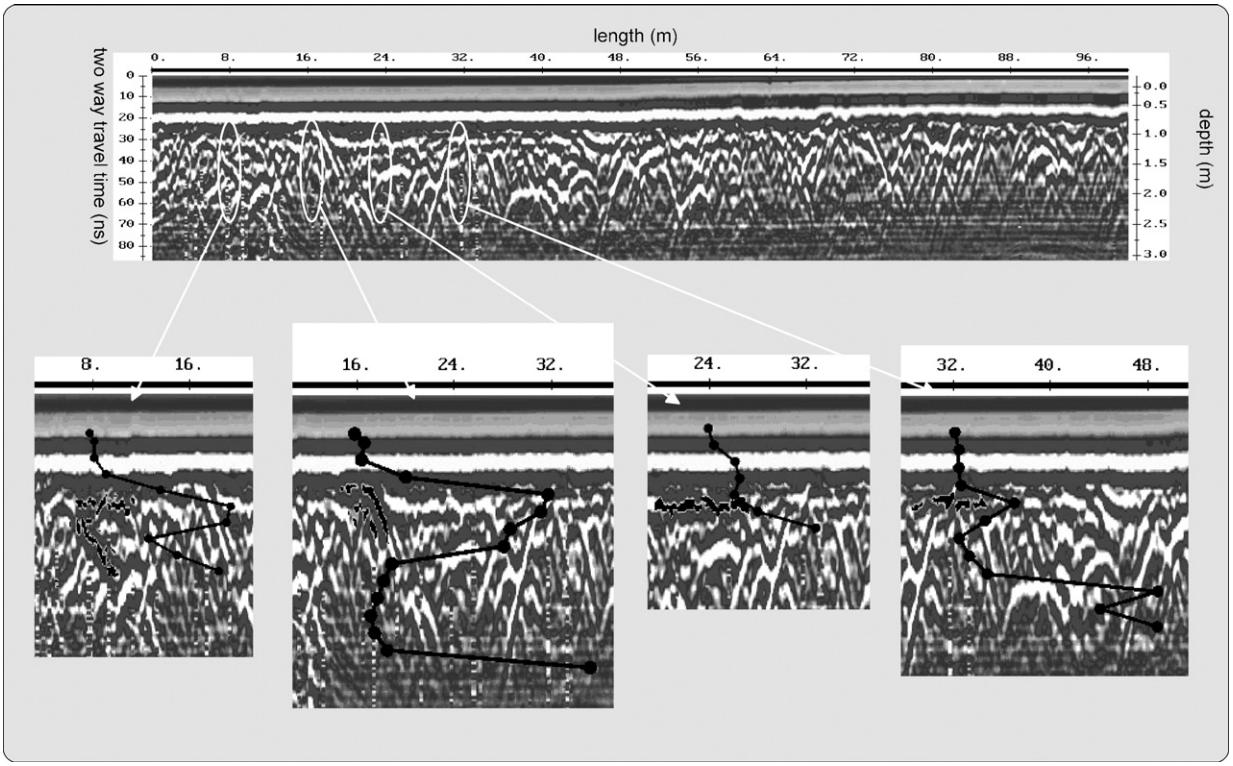

Fig. 11. Radar section at line 150 (200 MHz). The corresponding geotechnical tests are in red. (For interpretation of the references to colour in this figure legend, the reader is referred to the web version of this article.)

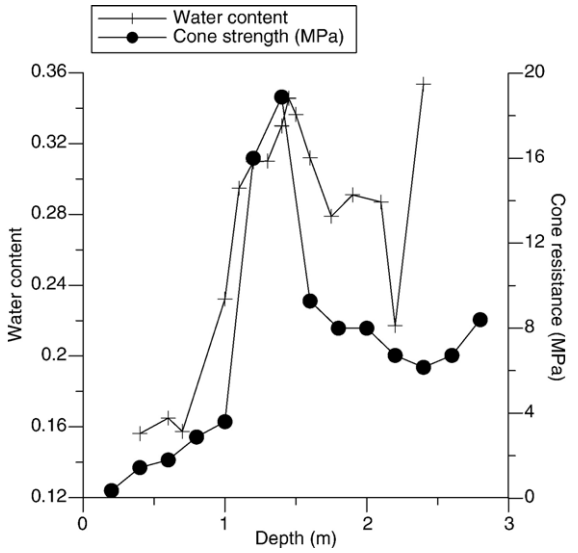

Fig. 12. Cone resistance and water content at line 25 as a function of depth.

produces the reflection drawn in blue in the GPR section.

It should be noted that this existence of the wet clayey soil, layer B in the geoelectrical model, has been also confirmed at line 25 by the seismic refraction survey with a 0.5 m geophone separation: an interface between a dry loose soil (350 m/s) and a wetter one (670–700 m/s) has been located at 0.9–1.5 m depth.

Fig. 11 shows numerous reflectors and diffractions which may have several origins: thin layers/pockets of gravels, heterogeneity of the water distribution, an irregular topography of the clayey soil (layer B)/limestone (layer C) interface. This statement is supported by the high amplitude of q_d and by the geological features of the site that we obtained previously. Some of these reflectors are correlated with peaks of resistance q_d but these correlations are rather weak compared to that observed at line 25 in Fig. 10. This point suggests that the layer A and B in the area of the line 25 would be less heterogeneous in comparison with the other studied areas. These poor correlations are also due to the fact that we applied a uniform velocity to GPR sections associated with a heterogeneous medium.

4. Quantitative correlations between electrical and geotechnical data

4.1. Interpreted resistivity vs. cone resistance

Since the comparison between electrical and geotechnical data provides satisfactory qualitative correlations, it was reasonable to investigate quantitative correlations. This first step was to study possible relationships between cone resistance values and interpreted resistivity values obtained from the ERT inversions.

In order to compare in a relevant way both parameters, two approaches have been considered. In a first approach, the cone resistance values are compared to the inverted resistivity values directly extracted from the grid given by RES2DINV. The resistivity values from the grid were interpolated linearly to the points (x,y,z) corresponding the q_d values from geotechnical tests.

Following the second approach, the cone resistance values are compared to the inverted resistivity values obtained from an inversion of 1D resistivity soundings extracted from the 2D apparent resistivity dataset. These 1D soundings were inverted 3 or 2 layer model, where the depth of each interface is determined from the geotechnical results. Indeed, the depth of each interface is fixed in the inversion process, in order to suppress the equivalences. The 1D inversions have been performed by a resolution of Hankel integral transform given by Guptasarma and Singh (1997).

The results given by the first and the second approach are given in Figs. 13 and 14 respectively. In both figures, the areas corresponding to the three layers geoelectrical model (i.e. layers A, B and C see Fig. 3) have been also drawn. In Fig. 13, the three areas have been defined from the layer thickness for each formation obtained from the geotechnical tests.

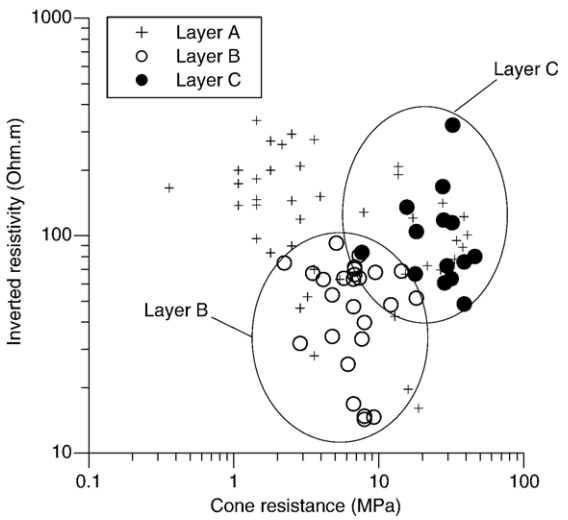

Fig. 13. Cone resistance vs inverted resistivity corresponding to the same location (x,y,z). Layer A: sands and gravels; Layer B: silts and Bourbonnais clays; Layer C: Jurassic Limestone (see Fig. 3).

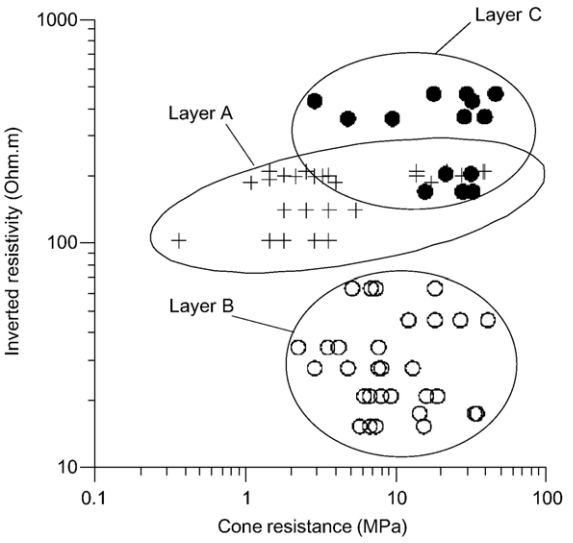

Fig. 14. Cone resistance vs. inverted resistivity extracted from 1D resistivity soundings.

In this analysis, we assumed that the high q_d peaks observed in line 150 were due to gravels: the corresponding q_d values were assigned to layer A i.e. sands and gravels. In Fig. 14, the uncertainty in interface depth estimate given by the geotechnical tests is about 20 cm. We checked the uncertainty does not modify the general picture given in Fig. 14.

If the whole set of couples (q_d, ρ) or the sets related to the three layers separately are considered, no quantitative correlation can be observed in Figs. 13 and 14: there is no bijective relationship between cone resistance and inverted resistivity. This result in agreement with a previous study (Braga et al., 1999) would not be surprising if only layer A had been investigated. Indeed, this geological unit contains on one hand very loose materials and on other hand, gravels; thus, the related cone resistance values are included in a very wide range as it is shown in Fig. 13.

Nevertheless, Figs. 13 and 14 show that couples (q_d, ρ) associated with layers B and C constitute two distinct populations. This distinction is better when inverted resistivity values from 1D soundings are considered (Fig. 14); in this particular case, the three formations, (i.e. layers A, B and C) can be better discriminated. This observation suggests that couple (q_d, ρ) would be a lithological discriminator in this particular site for the considered formations. This original result is not general but, in our opinion, similar analyses would deserve to be carried out in other sites with others lithologies.

4.2. Interpreted resistivity vs. water content

Electrical resistivity has been demonstrated to be an effective predictor of various soil properties including salinity (e.g. Rhoades et al., 1976), porosity and water content (e.g. Dannoski and Yaramanci, 1999; Tabbagh et al., 2002; Binley et al., 2002). That is why we examined a possible quantitative correlation between water content and inverted resistivity obtained from ERT sections.

Twenty soil samples have been collected each 10 cm depth from two in situ vane shear tests located at $x=9$ m $y=50$ m and $x=8.25$ m $y=150$ m and their gravimetric water content w have been measured from the usual oven-drying method at a 105 °C temperature. The first borehole located at $x=9$ m, $y=25$ m, 2.5 m deep, did not reach the layer C. The second and shortest borehole, 60 cm deep, located at $x=8.25$ m $y=150$ m did not reach the layer B. Consequently, the twenty soil samples are only associated with alluvial deposits (layer A and B).

In order to compare both parameters w and ρ, inverted resistivity values extracted from the grid given by RES2DINV was interpolated linearly to the points (x, y,z) corresponding the measured w values. Since the sample have been collected from only two boreholes with different lengths, the water content values have not been compared with the 1D inverted resistivity values extracted from 1D sounding.

The 2D inverted resistivity ρ and water content w corresponding to the same location (x,y,z) have been plotted in Fig. 15. Despite of the low number of points, a

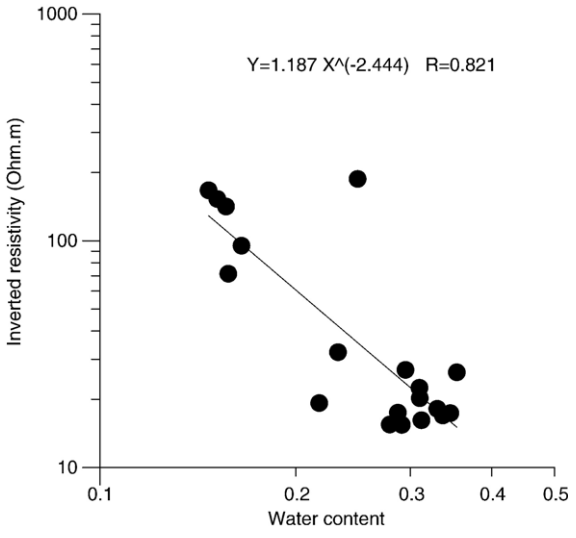

Fig. 15. Inverted resistivity as a function of measured water content.

satisfactory correlation between both properties has been obtained and the following empirical relationship can be proposed:

$$\rho = 1.187 w^{-2.444} \quad (3)$$

The scattering that can be observed in Fig. 15 may have several origins: (a) the resistivity values result from an interpolation of a 2D inversion; (b) several geological formations are concerned with different porosities and clay fractions.

Thus, it is difficult to compare these data with usual empirical laws linking resistivity (generally its inverse, electrical conductivity σ) and water content w, given in soil science literature (e.g. Rhoades et al., 1976; Mualem and Friedman, 1991). Important petrophysical parameters (porosity, electrical conductivity of the pore liquid) of the soils at the site are unfortunately unknown and a part of the soil column is clayey with likely a significant surface conductivity, which would have to be quantified. Nevertheless, it is interesting to note that the water content exponent 2.444 in our empirical equation is between 2, the exponent of Rhoades et al. law and 2.5, the exponent of Mualem and Friedman relationship. Consequently, our results do not seem to contradict usual σ–w relationships found in soil science literature.

5. Conclusion

The main objective of this study was to establish qualitative and quantitative correlations between electrical and geotechnical data collected in a site associated with a simple geological context. Concerning qualitative correlations, both approaches, geotechnical tests and ERT sections, suggest a three-layers model: a fine soil with a significant clay fraction sandwiched between an unsaturated sandy soil with gravels and the top of oolitic limestones. Despite the usual difficulty to point clearly interfaces in inverted ERT sections, both methods provide consistent depths of the substratum (i.e. limestones) top. On the basis of the geoelectrical model we proposed and the comparison with geotechnical data, this study confirms that ERT is a relevant method to determine clay cover in a subsurface context.

An attempt to obtain quantitative correlations has shown that a bijective relationship between cone resistance and inverted resistivity extracted from ERT sections and 1D soundings extracted from the same ERT sections does not exist. But, if we do not consider formation A, couple (ρ, q_d) would be a lithological discriminator. In addition, when inverted resistivity values obtained from 1D soundings are concerned, the discrimination of the different formations is enhanced. This observation should be validated in other sites.

Moreover, despite of the low number of data, a satisfactory quantitative correlation between inverted resistivity values and water content values has been obtained; this result demonstrates once more that resistivity is a good indirect predictor of water content.

Further projects should take into account other more powerful geotechnical tests (i.e. static cone penetration tests, standard penetration test and pressumeter) in other sites in order to investigate deeper depths associated with lithologies different than those in this study.

Acknowledgments

The authors thank H. Robain for his thoughtful comments that have improved the initial manuscript.

References

Abraham, O., Pedersen, H., Côte, Ph., 1998. Determination of shear velocity profiles for soil and concrete by analysis of seismic surface waves. 4th Meeting of Environmental and Engineering Geophysics, Barcelona, Expanded Abstract, pp. 343–347.

Binley, A., Cassiani, G., Middleton, R., Winship, P., 2002. Vadose zone flow model parameterisation using cross-borehole radar and resistivity imaging. Journal of Hydrology 267, 147–160.

Braga, A., Malagutti, W., Dourado, J., Chang, H., 1999. Correlation of electrical resistivity and induced polarization data with geotechnical survey standard penetration test measurements. Journal of Environmental and Engineering Geophysics 4, 123–130.

Dannoski, G., Yaramanci, U., 1999. Estimation of water content and porosity using combined radar and geoelectrical measurements. European Journal of Environment and Engineering Geophysics 4, 71–85.

De Groot-Hedlin, C., Constable, S., 1990. Occam's inversion to generate smooth, two dimensional models from magnetotelluric data. Geophysics 55, 1613–1624.

Edwards, L.S., 1977. A modified pseudosection for resistivity and IP. Geophysics 42 (5), 1020–1036.

Endres, A.L., Clement, W.P., 1998. Relating cone penetrometer test information to geophysical data: a case study. Symposium on the Application of Geophysics to Engineering and Environmental Problems (SAGEEP98). Chicago. USA.

Filliat, G., 1981. La pratique des sols et fondations. Moniteur Ed, Paris.

Ghose, R., Drijkoningen, G.G., 2000. Interacting soil-physical parameters in the cone penetration process in sand: scope of integration of seismic to CPT. 6th Meeting of Environmental and Engineering Geophysics, Bochum, Expanded Abstract, vol. EG02.

Giao, P.H., Chung, S.G., Kim, D.Y., Tanaka, H., 2003. Electrical imaging and laboratory resistivity testing for geotechnical investigation of Pusan clay deposits. Journal of Applied Geophysics 52, 157–175.

Guptasarma, D., Singh, B., 1997. New digital linear filters for Hankel J_0 and J_1 transforms. Geophysical Prospecting 45, 745–762.

Lagabrielle, R., Palma Lopes, S., Toe, E., Nikodic, J., 2000. Alluvium resistivity survey under sea water for the new harbour of La Havre (France). 6th Meeting of Environmental and Engineering Geophysics, Bochum, Expanded Abstract, vol. EL10.

Menot, J.C., Debrand-Passard, S., Clozier, L., Gros, Y., 1997. Notice explicative de la feuille La Charité-sur-Loire à 1/50000. Bureau de Recherches Géologiques et Minières Ed. Orléans, France.

Meyer De Stadelhofen, C., 1991. Applications de la géophysique aux recherches d'eau. Lavoisier Ed. Paris, France.

Mualem, Y., Friedman, S.P., 1991. Theoretical prediction of electrical conductivity in saturated and unsaturated soil. Water Resources Research 27, 2771–2777.

Nauroy, J.-F., Dubois, J.-C., Colliat, J.-L., Kervadec, J.-P., Meunier, J., 1998. The GEOSIS method for integrating VHR seismic and geotechnical data in offshore site investigations. Conf. on Offshore Site Investigation and Foundation Behaviour, September, Londres, United-Kingdom, vol. 1, pp. 150–162.

Puech, A., Brel, D., Magnin, O., Rivoallan, X., 2000. An integrated marine geophysical and geotechnical survey for the "Port 2000" extension project in Le Havre. 6th Meeting of Environmental and Engineering Geophysics, Sept. 3–7, Bochum, Expanded Abstract, vol. CH03.

Rhoades, J.D., Ratts, P.T.C., Prather, R.J., 1976. Effects of liquid phase electrical conductivity, water content and surface conductivity on bulk soil electrical conductivity. Soil Science Society of America Journal 40, 651–655.

Tabbagh, A., Benderitter, Y., Michot, D., Panissod, C., 2002. Measurement of variations in soil electrical resistivity for assessing the volume affected by plant water uptake. European Journal of Environmental and Engineering Geophysics 7, 229–237.

Venkatramaiah, C., 1993. Geotechnical Engineering. John Wiley & Sons, New Delhi, India.

Vickery, A., Hobbs, B., 2003. Resistivity imaging to determine clay cover and permeable units at an ex-industrial site. Near Surface Geophysics 1, 131–137.